# Temperature and Time Dependence of Electrical Resistivity in an Anisotropically Conductive Polymer Composite with *In Situ* Conductive Microfibrils

**Yi-Chuan Zhang, Kun Dai, Huan Pang, Qiao-Ji Luo, Zhong-Ming Li, Wei-Qin Zhang**

*College of Polymer Science and Engineering, State Key Laboratory of Polymer Materials Engineering, Sichuan University, Chengdu 610065, Sichuan, People's Republic of China*

Received 5 August 2010; accepted 7 July 2011
DOI 10.1002/app.35193
Published online 21 October 2011 in Wiley Online Library (wileyonlinelibrary.com).

**ABSTRACT:** An anisotropically conductive polymer composite (ACPC) based on conductive carbon black (CB) and binary polymer blend of polyethylene (PE) and polyethylene terephthalate (PET) was successfully fabricated under shear and elongational flow fields. The PET phase formed *in situ* the aligned conductive microfibrils whose surfaces were coated by CB particles. This ACPC material exhibited a strong electrical anisotropy within a broad temperature range. When the ACPC samples were subjected to isothermal treatment (IT), they showed anomalous variations of the positive temperature coefficient (PTC) and negative temperature coefficient (NTC) effects. The PTC intensity was attenuated gradually with the increase of the IT time, and the NTC intensity was nearly eliminated after IT of 8 or 16 h. Beyond 16 h, the resistivity in the NTC region rose anomalously with the temperature after the elimination of NTC effect, which was the result of much transformation from the potential pathways to the intrinsic pathways due to the disordering of oriented conductive microfibrils. When the amount of potential pathways was very small, the effect of the intrinsic pathway separation surmounts that of the potential pathways, leading to the anomalous resistivity increase in the NTC region. © 2011 Wiley Periodicals, Inc. J Appl Polym Sci 124: 1808–1814, 2012

**Key words:** electrical properties; microfibrillar blend; conductive polymer composites; electrical anisotropy

## INTRODUCTION

An anisotropically conductive polymer composite (ACPC), by definition, has much higher conductivity in one direction than that in the others. ACPC has currently drawn considerable attention because of its unique electrical properties and potential applications such as field emission devices and electronic sensors.[1–3] The alignment of conductive fillers in a polymer matrix is the precondition of ACPC fabrication. Some approaches have been proposed for the preferential alignment of conductive fillers, which basically utilize external fields including electrical field, magnetic field, and mechanical force, etc.[3–12] Tai et al.[3] prepared carbon black (CB) filled ACPC under isothermal treatment in an electric field of 500 V/mm. Kimura et al.[4] offered magnetic field inducing alignment of carbon nanotubes (CNTs) in the polyester matrix. Xu et al.[7] suggested that shear flow brought the alignment of CNTs in epoxy composites.

Conductive polymer composites often exhibit two major physical phenomena, positive temperature coefficient (PTC) effect and negative temperature coefficient (NTC) effect, which are the sharp increase and the succeeding gradual decrease of the resistivity around the melting point of the matrix polymer, respectively. They reflect the change of the microstructure of the conductive composites upon elevated temperature. Many models, such as volume expansion, conduction pathway theory and tunneling effect theory, etc., have been proposed to interpret PTC and NTC effects,[13–17] but their origin is still in dispute up to the present. Most works about PTC and NTC are focused on the isotropic conductive network existent in the isotropically conductive polymer composite (ICPC).[18–20] From the thermodynamic point of view, the response of isotropic conductive network is relatively inert to temperature. In contrast, ACPC has anisotropic conductive network composed of aligned conductive components. The interaction between macromolecular chains and aligned conductive components is sensitive to the temperature variation, thus producing a strong electric signal, manifesting the microstructural variations of anisotropic conductive network in different

Additional Supporting Information may be found in the online version of this article.

*Correspondence to:* Z.-M. Li (zm_li@263.net.cn).

Contract grant sponsor: National Outstanding Youth Foundation of China; contract grant number: 50925311.

directions. Accordingly, it may help interpret the origin of PTC and NTC by temperature-conductivity behavior of ACPC.

In our previous work,[21] shear and elongational flow fields were used to achieve the alignment of conductive components (CB coated polymer microfibrils) and fabricate a unique ACPC based on CB particles, poly(ethylene terephthalate) (PET) and polyethylene (PE). In this ACPC material, the majority of CB particles were localized in the surface region of *in situ* formed, aligned PET microfibrils. The resultant ACPC exhibited a strong anisotropy in conductivity due to the oriented conductive microfibrils. The present work measured the temperature and time dependence of electrical resistivity of the obtained ACPC samples. The origin of PTC and NTC effect was discussed depending on the structural development of the anisotropic conductive microfibrillar network.

## EXPERIMENTAL

### Materials

The main materials used in this work include electrically conductive CB, high density PE, and PET. The CB, model VXC-605, from Cabot, with a dibutyl phthalate (DBP) absorption value of 148 ± 15 $cm^3$/100 g, was dried at 120°C for 10 h to get rid of the water before use. PE is 5000S, a commercial high-density PE of Daqing Petroleum Chemical, Daqing, China, and its melt flow rate is 0.9 g/10 min at 190°C, exerting a load of 21.6*N*, and its number average molecular weight is 5.3 × $10^5$ g/mol. PET was friendly donated by Luoyang Petroleum Chemical, Luoyang, China, which is a commercial grade of textile polyester with a number average molecular weight of ca. 2.3 × $10^4$ g/mol.

### Preparation of the ACPC

CB particles and PE pellets were first melt mixed in an internal mixer. The thus obtained compound was granulated and further melt mixed with PET via extrusion. The weight ratio of PET and PE is 3 : 7. The obtained composite was extruded through a slit die and then subjected to post hot stretching and quenching. The schematic illustration about the architecture of the resultant ACPC is shown in Figure 1. Details about the morphological description and percolation behavior were available in the Supporting Information.

### Resistivity-temperature behaviors test

In the resistivity-temperature test, copper electrodes were attached to the cross sections of a sample in the parallel direction with silver paint. The sample

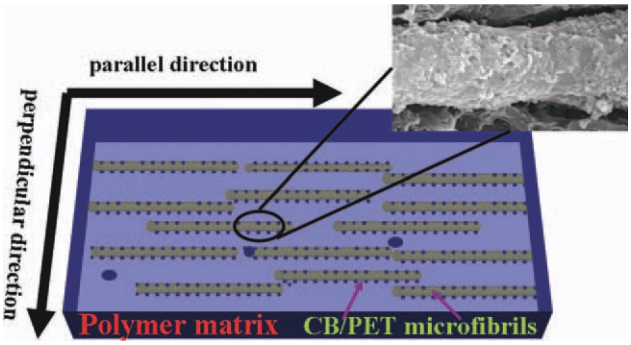


**Figure 1** Schematic illustration about the architecture of the resultant composite. [Color figure can be viewed in the online issue, which is available at wileyonlinelibrary.com.]

was immersed in silicone oil of a temperature-controlled apparatus to avoid oxidation. The thermal procedure of the sample for resistivity-temperature test is: heated from 20 to 180°C at 2°C/min and held at this temperature for 3 min, then cooled to 20°C at the same rate. The data were recorded by a computer. After the test of sample in the parallel direction, another sample was measured in the perpendicular direction with the same test method. To explore the influence of the thermal treatment, some samples were annealed at 180°C for different time (2, 8, 16, 32, and 46 h). For the sake of brevity, isothermal treatment at 180°C is referred to IT.

### Thermal property test

Thermal analyses were carried out by a Netzsch DSC 204 differential scanning calorimeter. The samples were heated to 180°C at 2°C/min, kept for 3 min, and then cooled at 2°C/min to 20°C, a heating-cooling journey matching resistivity-temperature tests.

### Two-dimensional wide angle X-ray diffraction

A two-dimensional wide-angle X-ray diffraction (2D-WAXD) was employed to characterize the orientation of PE crystallites in the parallel direction. The incident X-ray beam was set perpendicular to the surface of sample with 1 mm thickness. The measurement was carried on the synchrotron light source (wavelength, $\lambda = 0.15498$ nm) with the MarCCD as the detector at National Synchrotron Radiation Laboratory, Hefei, China. The orientation parameter was calculated mathematically using Picken's method from the (110) WAXD reflection for PE.[22]

## RESULTS AND DISCUSSION

### Anisotropy of resistivity-temperature behavior

Figure 2 shows the resistivity-temperature behavior of the ACPC samples, which presents a strong

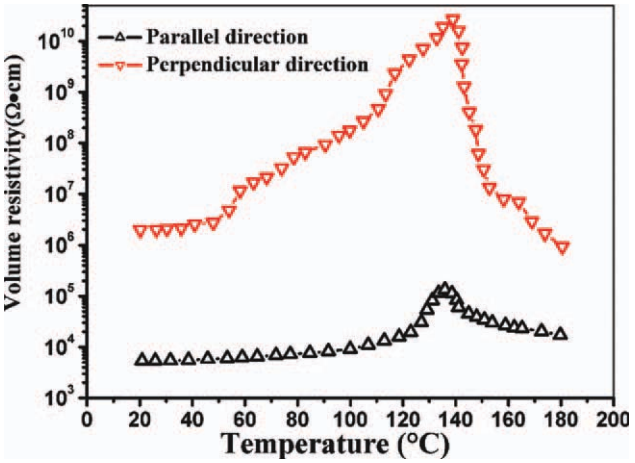


**Figure 2** Resistivity-temperature relationships of the ACPC samples with 4.93 vol % content of CB. [Color figure can be viewed in the online issue, which is available at wileyonlinelibrary.com.]

anisotropy within a board temperature range from 20 to 180°C. Like the conventional conductive polymer composite, the ACPC samples also exhibit two basic features, PTC and NTC effects. To evaluate the PTC and NTC effects quantitatively, the PTC and NTC intensities are defined as

$$I_{\mathrm{PTC}} = \log\left(\frac{\rho_t}{\rho_{RT}}\right)$$

$$I_{\mathrm{NTC}} = \log\left(\frac{\rho_{\max}}{\rho_k}\right)$$

where $\rho_t$ is the maximum resistivity in PTC region, $\rho_{RT}$ is the original resistivity at 20°C, $\rho_{\max}$ is the maximum resistivity in the whole heating process, and $\rho_k$ is the resistivity at the given temperature $k$ after PTC region, that is, 180°C in the present study. Using this definition, the ACPC sample has a low $I_{\mathrm{PTC}}$, only 1.40, in the parallel direction, compared with a $I_{\mathrm{PTC}}$ of 4.13 in the perpendicular direction, as shown in Figure 2. This difference in PTC effect is attributed to conductive network structure. In the parallel direction, there are numerous conductive pathways formed via fine contacts of aligned conductive microfibrils, which are hard to break. While in the perpendicular direction, the conductive pathways are basically constructed via the transfer of electrons between conductive microfibrils and a few CB particles left in the matrix. The amount of CB particles is very limited and the microfibrils are intrinsically aligned in the parallel direction, as a result, compared to the parallel direction, there are much less conductive pathways in the perpendicular direction. As the temperature increases to the melting temperature ($T_m$) of PE (see DSC curves in Fig. 3), melting of the PE crystallites produces a sharp volume increase, and causes separation of the conductive pathways, giving rise to PTC effect. However, due to perfectly formed conductive pathways in the parallel direction, breakup of a fraction of pathways has less influence on conductivity, the PTC effect in this direction is thus very weak compared to that in the perpendicular direction.

With the increase of temperature beyond $T_m$ of PE, the resistivity of ACPC gradually decreases, exhibiting the so-called NTC effect. The NTC intensity is 0.89 in the parallel direction, while up to 4.45 in the perpendicular direction. In spite of the big size of the conductive PET microfibrils, the interaction of polar groups and the large specific surface area of CB particles can still drive the conductive microfibrils to gradually agglomerate in the melting PE.[23–25] Based on the tunneling mechanism proposed by Balberg et al.,[26–28] the minute increase of the distance between conductive components results in an obvious increase of the resistivity, and *vice versa*. With the PET microfibrils aggregated in the PE melt, the distance between conductive microfibrils diminishes gradually, which leads to the significant reduction of resistivity. That is to say, many new conductive pathways are formed in the PE melt due to the aggregation of conductive microfirbils, which is responsible for the strong NTC effect in the perpendicular direction. In contrast, there are many pre-existing conductive pathways above $T_m$ in the parallel direction. The newly formed conductive pathways only intensify pre-existing pathways to some extent and do not improve conductivity significantly, giving rise to a low NTC effect.

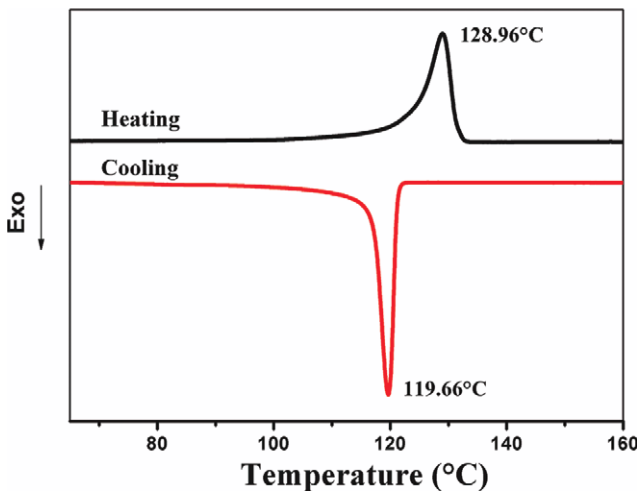


**Figure 3** DSC curves of the ACPC samples with 4.93 vol % content of CB during heating and cooling. [Color figure can be viewed in the online issue, which is available at wileyonlinelibrary.com.]

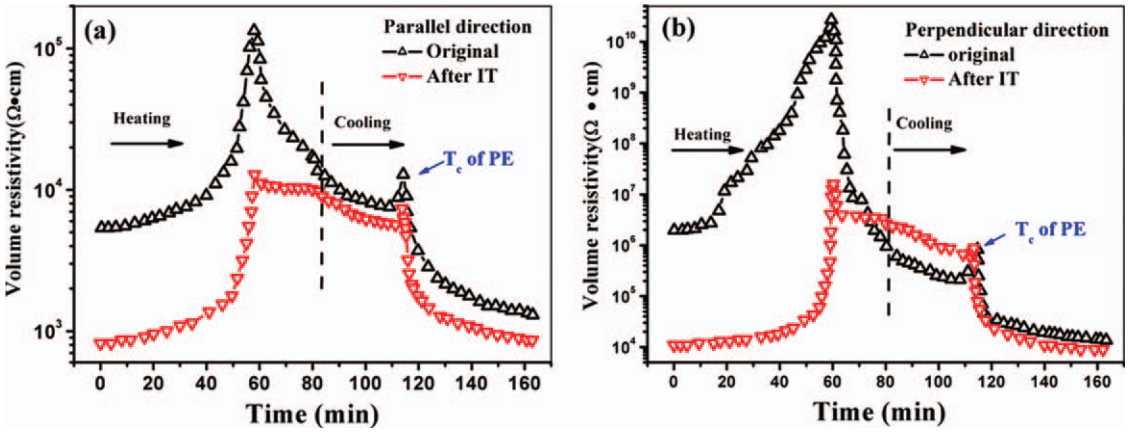


**Figure 4** Time dependence of resistivity of the original ACPC sample and the ACPC sample after IT in the parallel (a) and perpendicular (b) directions. [Color figure can be viewed in the online issue, which is available at wileyonlinelibrary.com.]

### Attenuation of PTC and NTC effect after IT

Figure 4 shows the time dependence of the resistivity of the original ACPC sample and the isothermally treated ACPC sample during heating and cooling (for easy understanding, the temperature is changed to time scale here). It is interesting that, after IT of 2 h, $I_{PTC}$ and $I_{NTC}$ are attenuated in both directions. In the parallel direction, $I_{PTC}$ and $I_{NTC}$ reduce from 1.40 and 0.89 to 1.19 and 0.10 [Fig. 4(a)], respectively; in the perpendicular direction, $I_{PTC}$ and $I_{NTC}$ from 4.14 and 4.45 to 3.16 and 0.77 [Fig. 4(b)], respectively. The microstructural changes and large size of the conductive microfibrils can account for the attenuation of $I_{PTC}$ and $I_{NTC}$. The oriented conductive microfibrils in PE matrix are not thermodynamically stable, and they tend to disorder to increase entropy.[29–31] The unique oriented conductive structure is frozen and stabilized by quenching in cold water during the preparation of ACPC. Once the temperature exceeds $T_m$ of PE, the low viscous PE melt provides favorable conditions for aligned microfibrils to disorder by Brownian movement. In particular, this irregular movement is strengthened by the large specific surface area of CB particles and the interaction between polar groups on the microfibrils' surface.

Based on the above analysis, a model as shown in Figure 5 is proposed to explain the evolution of the electrical pathways in both directions. Figure 5(a) displays the original state of ACPC. Most of aligned conductive microfibrils are well isolated by PE layers, which create highly anisotropic conductivity. The overlapping conductive microfibrils are defined as the intrinsic pathways, and the isolated ones are defined as the potential pathways which can be transformed into the intrinsic pathways through the disordering of conductive microfibrils. After the first heating-cooling run, some potential pathways disorder above $T_m$ of PE and transform into intrinsic pathways via Brownian movement, as shown in Figure 5(b). In Figure 5(c), more transformation to the intrinsic pathways from the potential pathways occurs on account of the further disordering of conductive microfibrils after IT of 2 h. In other words, ACPC obtains better conductivity due to generation

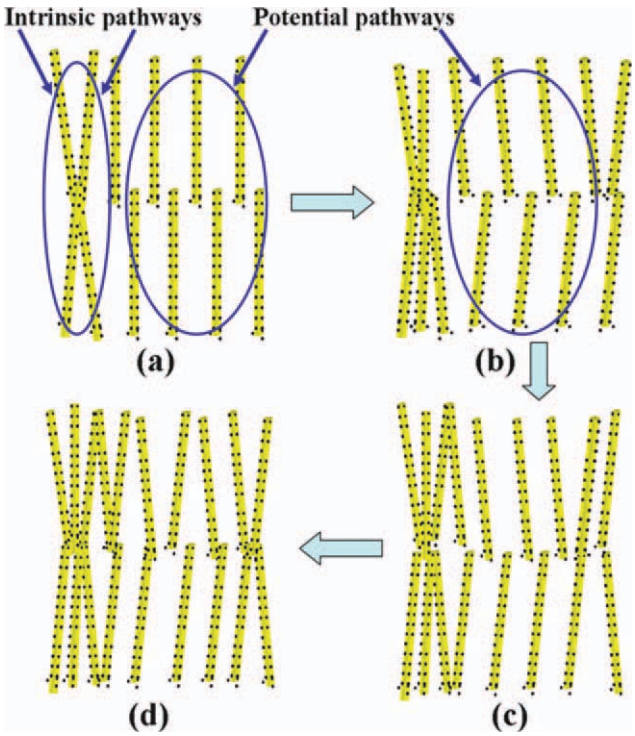


**Figure 5** Schematic illustration of the evolution of the electrical pathways during thermal treatment of different period: (a) the original state; (b) conductive network after the first heating-cooling run; (c) conductive network after IT of 2 h; and (d) conductive network after the second heating-cooling run. [Color figure can be viewed in the online issue, which is available at wileyonlinelibrary.com.]

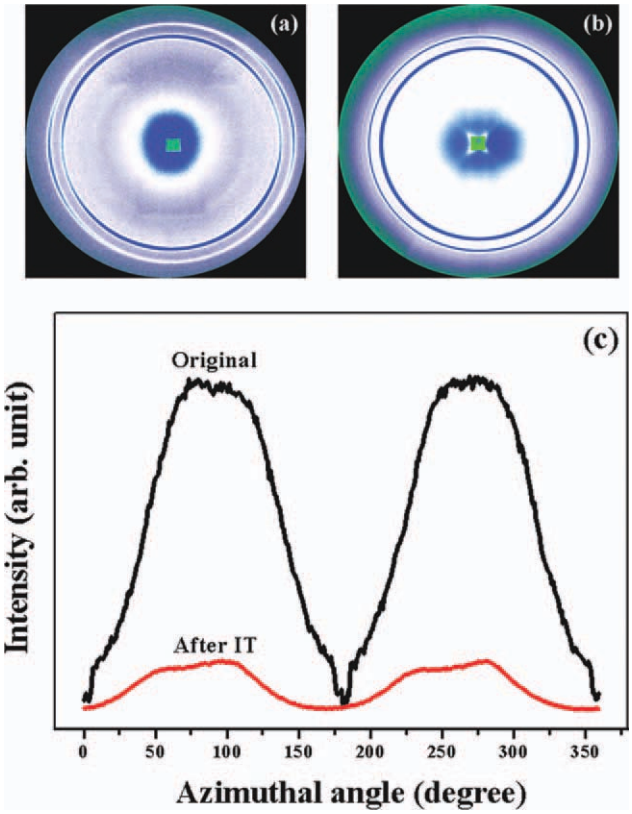


**Figure 6** 2-D WAXD patterns of sample strip in the original ACPC sample (a) and the ACPC sample after IT (b), respectively. The (110) intensity distribution along the azimuth angle (c). [Color figure can be viewed in the online issue, which is available at wileyonlinelibrary.com.]

of more intrinsic pathways.[32] Hence, separation and aggregation of a fraction of intrinsic pathways has less effect on conductivity. That is why the ACPC sample after IT of 2 h displays weak PTC and NTC effects (Fig. 4). After the second heating-cooling run, the number of potential pathways is small as shown in Figure 5 days, which implies weaker PTC and NTC effects after longer IT time.

Further validity of this model needs to testify the disordering of aligned conductive microfibrils in the IT process. The direct data about the conductive microfibrils' disordering are unavailable at present. Alternatively, we characterize the molecular orientation degree of PE in the original ACPC sample and the isothermally treated ACPC sample, as shown in Figure 6. The 2D-WAXD patterns of the original ACPC sample show that the Bragg intensity is preferentially concentrated in two opposite directions [Fig. 6(a)]. However, the Bragg intensity is uniformly distributed after IT [Fig. 6(b)]. The actual intensity distribution along the azimuthal angle of the (110) is shown in Figure 6(c). Two peaks are found centered at about $\Phi = 90$ and 270° in the original sample, and the peaks disappear after IT. By Picken's method,[22] the orientation degree of PE crystals is about 0.21 in the original sample, while there is almost no PE molecular orientation after IT. The disappearance of the PE molecular orientation can indirectly verify the disordering of the oriented conductive microfibrils in the IT process. The unique hot stretching-quenching technique is responsible for formation of oriented conductive microfibrils. Shear and elongational flow imposed on the PE melt makes the droplets of dispersed phase (PET) deform and therefore forms aligned microfibrils.[33] Wu et al.[24,25] suggested the mobility of polymer layer surrounding CB actually reflected the mobility of CB particles in the matrix because the contact process of two CB particles was equivalent to the excluding process of the macromolecular chains between two CB particles. From this point of view, the orientation degree of PE crystals can reflect the resultant orientation of the PET microfibrils. It needs to be noted that the orientation degree of PE is not high. This can be ascribed to the low stretch ratio and the fast relaxation of PE chains. It is well-known that the PE chains relax easily due to their highly flexible chains. The PE chains largely relax in the interval between hot stretching and quenching. However, the high alignment of PET microfibrils can be well preserved due to their large size. During IT, the oriented PE chains relax into random coils, which stimulate the disordering movement of the conductive microfibrils. During cooling, PE chains rearrange to form unoriented crystals, and the disordering conductive microfibrils are finally frozen in a less degree of alignment.

During cooling, the resistivity decreases slowly with temperature above the crystallization temperature ($T_c$) of PE (see DSC in Fig. 3). Around $T_c$ of PE, a low resistivity peak appears in the original ACPC sample [Fig. 4(a,b)], but just below $T_c$ of PE, it shows a sharp decrease. This phenomenon is very similar to PTC and NTC effects during heating, and accordingly, the increase and decrease of resistivity are called the cooling PTC and NTC, respectively.[34] It is found that the cooling PTC effect in Figure 4(a,b) is relatively low in contrast to that of ICPC in our previous work.[35] When the temperature reduces to $T_c$, many conductive contacts between the intrinsic pathways are separated by tiny crystalline grains, resulting in sharp increase of resistivity.[36,37] In the meanwhile, the potential pathways continue disordering to bring higher conductivity, which compensates the conductivity loss for the separating conductive contacts.[32] Accordingly, low cooling PTC effects occur in Figure 4(a,b). Whereafter, the distance between the intrinsic pathways is diminished because of the rapid volume shrinkage of crystallization, which is responsible for the cooling NTC below $T_c$.

More intensified IT (i.e., longer IT time) is imposed on the ACPC samples to reveal their resistivity-temperature relationship as shown in Figure 7.

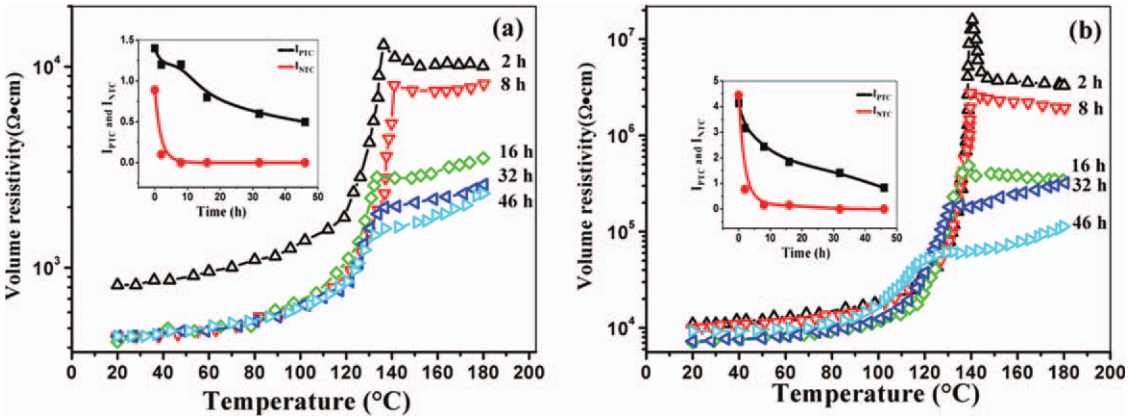


**Figure 7** The volume resistivity-temperature behaviors of the ACPC sample in the parallel (a) and perpendicular (b) directions after different IT time (2, 8, 16, 32, and 46 h). The inset shows the IT time dependence of $I_{PTC}$ and $I_{NTC}$. [Color figure can be viewed in the online issue, which is available at wileyonlinelibrary.com.]

It is found that, with the increase of the IT time, the PTC intensity is attenuated by degrees in both directions, while the NTC intensity is weakened dramatically, even is nearly eliminated after 8 h in the parallel direction, or 16 h in the perpendicular direction. Surprisingly, after 32 and 46 h, not only is the NTC intensity eliminated completely, but also the resistivity rises anomalously with the temperature; even the resistivity exceeds the resistivity around $T_m$ of PE. To the best of our knowledge, this interesting phenomenon has never been reported in the available literature. To explain this interesting phenomenon, we take the transformation between the intrinsic pathways and the potential pathways into account. The potential pathways which are originally isolated by PE layers cannot disorder to form the intrinsic pathways until the temperature approaches $T_m$ of PE. As a result, the potential pathways are not responsible for PTC effect during heating. In other words, PTC effect is only ascribed to the intrinsic pathways. Beyond $T_m$ of PE, the potential pathways start to take effect in building conductive networks, meanwhile, a small amount of intrinsic pathways separate each other due to linear thermal expansion of volume. Therefore, the NTC effect is dominated by the combined influence of intrinsic and potential pathways.

The relatively perfect conductive network is formed through transformation from the potential pathways to intrinsic ones during IT. The conductive network cannot be broken easily due to the existence of large numbers of intrinsic pathways during heating, which results in the gradual decrease of the PTC intensity as observed in Figure 7. It is noted that the number of potential pathways is large, and the resistivity in the NTC region varied with the number of the potential pathways. On one hand, the disordering of the potential pathways is in favor of conductivity. On the other hand, the separation of the intrinsic pathways, owing to the volume linear thermal expansion, goes against conductivity. There is a competitive process. The effect of the intrinsic pathway separation after $T_m$ of PE can be neglectable when the potential pathways exist in a great number, as revealed by strong NTC effects in Figure 2. Nevertheless, the number of potential pathways reduces dramatically with the IT time. A critical balance between disordering of the potential pathways and separation of the intrinsic pathways is stricken when the number of potential pathways reduces to a certain critical point; under the circumstance, the elimination of NTC effects appears. With further reduction of the number of potential pathways, the effect of the intrinsic pathway separation surmounts that of the potential pathways, leading to the anomalous increase of resistivity in NTC region after IT of 32 and 46 h.

## CONCLUSION

The ACPC material with *in situ* conductive microfibrils exhibits a strong electrical anisotropy within a broad temperature range from 20 to 180°C. The different topological structure of the conductive network is responsible for the different PTC and NTC effects between the parallel and perpendicular directions. After IT of 2 h, $I_{PTC}$ and $I_{NTC}$ are attenuated in both directions. Much transformation from the potential pathways to the intrinsic pathways occurs on account of the disordering of microfibrils. The existence of a large number of intrinsic pathways causes the attenuation of $I_{PTC}$ and $I_{NTC}$ after IT of 2 h in both directions. The cooling PTC effect is relatively low in contrast to that in the ICPC, because the disordering of PET microfibrils compensates conductivity for the separating conductive contacts due to the crystallization. $I_{PTC}$ decreases gradually with the IT time. The resistivity in NTC

region varies with the number of the potential pathways. When the number of the potential pathways is very small, the anomalous increase of resistivity in NTC region occurs after IT of 32 and 46 h. Our results can help understand the response of anisotropic conductive network to the variation of temperature field.

## References


1. Yoshio, M.; Kagata, T.; Hoshino, K.; Mukai, T.; Ohno, H.; Kato, T. J Am Chem Soc 2006, 128, 5570.
2. Gao, J. F.; Yan, D. X.; Yuan, B.; Huang, H. D.; Li, Z. M. Compos Sci Technol 2010, 70, 1973.
3. Tai, X. Y.; Wu, G. Z.; Tominaga, Y.; Asai, S.; Sumita, M. J Polym Sci Part B Polym Phys 2005, 43, 184.
4. Kimura, T.; Ago, H.; Tobita, M.; Ohshima, S.; Kyotani, M.; Yumura, M. Adv Mater 2002, 14, 1380.
5. Zoldan, J.; Siegmann, A.; Narkis, M. Polym Eng Sci 2006, 46, 1250.
6. Lu, J. R.; Weng, W. G.; Chen, X. F.; Wu, D. J.; Wu, C. L.; Chen, G. H. Adv Funct Mater 2005, 15, 1358.
7. Xu, J. W.; Florkowski, W.; Gerhardt, R.; Moon, K. S.; Wong, C. P. J Phys Chem B 2006, 110, 12289.
8. Lanticse, L. J.; Tanabe, Y.; Matsui, K.; Kaburagi, Y.; Suda, K.; Hoteida, M.; Endo, M.; Yasuda, E. Carbon 2006, 44, 3078.
9. Martin, C. A.; Sandler, J. K. W.; Windle, A. H.; Schwarz, M. K.; Bauhofer, W.; Schulte, K.; Shaffer, M. S. P. Polymer 2005, 46, 877.
10. Zhu, Y. F.; Ma, C.; Zhang, W.; Zhang, R. P.; Koratkar, N.; Liang, J. J Appl Phys 2009, 105, 054319.
11. Ma, C.; Zhang, W.; Zhu, Y. F.; Ji, L. J.; Zhang, R. P.; Koratkar, N.; Liang, J. Carbon 2008, 46, 706.
12. Dombovari, A.; Halonen, N.; Sapi, A.; Szabo, M.; Toth, G.; Mäklin, J.; Kordas, K.; Juuti, J.; Jantunen, H.; Kukovecz, A.; Konya, Z. Carbon 2010, 48, 1918.
13. Kohler, F. U.S. Pat. 1966, 3,243,753.
14. Ohe, K.; Natio, Y. Jpn J Appl Phys 1971, 10, 99.
15. Meyer, J. Polym Eng Sci 1974, 14, 706.
16. Voet, A. Rubber Chem Technol 1981, 54, 42.
17. Klason, C.; Kubat, J. J Appl Polym Sci 1975, 19, 831.
18. Jeevananda, T.; Kim, N. H.; Lee, J. H.; Basavarajaiah, S.; Ursd, M. V. D.; Ranganathaiahd, C. Polym Int 2009, 58, 775.
19. Dang, Z. M.; Li, W. K.; Xu, H. P. J Appl Phys 2003, 106, 024913.
20. Mironi-Harpaz, I.; Narkis, M. J Polym Sci Part B Polym Phys 2001, 39, 1415.
21. Zhang, Y. C.; Dai, K.; Tang, J. H.; Ji, X.; Li, Z. M. Mater Lett 2010, 64, 1430.
22. Picken, S. J.; Aerts, J.; Visser, R.; Northolt, M. G. Macromolecules 1990, 23, 3849.
23. Xu, X. B.; Li, Z. M.; Dai, K.; Yang, M. B. Appl Phys Lett 2006, 89, 032105.
24. Wu, G. Z.; Asai, S.; Sumita, M. Macromolecules 2002, 35, 1708.
25. Wu, G. Z.; Asai, S.; Zhang, C.; Miura, T.; Sumita, M. J Appl Phys 2000, 88, 1480.
26. Balberg, I.; Azulay, D.; Toker, D.; Millo, O. Int J Mod Phys B 2004, 2091, 18.
27. Grimaldi C.; Balberg, I. Phys Rev Lett 2006, 96, 066602.
28. Rubin, Z.; Sunshine, S. A.; Heaney, M. B.; Bloom, I.; Balberg, I. Phys Rev B 1999, 59, 12196.
29. Li, B.; Zhang, Y. C.; Li, Z. M.; Li, S. N.; Zhang, X. N. J Phys Chem B 2010, 114, 689.
30. Deng, H.; Zhang, R.; Reynolds, C. T.; Bilotti, E.; Peijs, T. Macromol Mater Eng 2009, 294, 749.
31. Deng, H.; Skipa, T.; Bilotti, E.; Zhang, R.; Lellinger, D.; Mezzo, L.; Fu, Q.; Alig, I.; Peijs, T. Adv Funct Mater 2010, 20, 1424.
32. Balberg I.; Binenbaum, N. Phys Rev B 1983, 28, 3799.
33. Li, Z. M.; Li, L. B.; Shen, K. Z.; Yang, M. B.; Huang, R. J Polym Sci Part B Polym Phys 2004, 42, 4095.
34. Xu, S. X.; Wen, M.; Li, J.; Guo, S. Y.; Wang, M.; Du, Q.; Shen, J. B.; Zhang, Y. Q.; Jiang, S. L. Polymer 2008, 49, 4861.
35. Dai, K.; Li, Z. M.; Xu, X. B. Polymer 2008, 49, 1037.
36. Alig, I.; Lellinger, D.; Dudkin, S. M.; Pötschke, P. Polymer 2007, 48, 1020.
37. Deng, H.; Skipa, T.; Zhang, R.; Lellinger, D.; Bilotti, E.; Alig, I.; Peijs, T. Polymer 2009, 50, 3747.